

Coincidence measurement of the fully differential cross section for atomic-field bremsstrahlung*

J. D. Faulk and C. A. Quarles

Department of Physics, Texas Christian University, Fort Worth, Texas 76129

(Received 23 February 1973)

A coincidence measurement of the absolute cross section for electron-atomic-field bremsstrahlung, differential in photon energy, photon-emission angle, and electron scattering angle, is reported. The incident electron energy was 140 keV and the scattering materials were thin films of aluminum and gold. Measurements were made for the following cases of electron scattering angle (θ_{ei}), photon-emission angle ($\theta_{\gamma i}$), and photon energy (k): $\theta_{ei}=15^\circ$, $\theta_{\gamma i}=270^\circ$, and $k=30$ and 70 keV; $\theta_{ei}=30^\circ$, $\theta_{\gamma i}=270^\circ$, and $k=20$ and 70 keV; and $\theta_{ei}=30^\circ$, $\theta_{\gamma i}=30^\circ$, and $k=20, 30, 50,$ and 70 keV. The data are compared to the theoretical calculations of Elwert and Haug and of Bethe and Heitler. Both theories give generally satisfactory agreement for aluminum. The Elwert-Haug theory is somewhat more accurate for gold, although neither theory agrees with the data at $\theta_{\gamma i}=270^\circ$ and $k=70$ keV. A discrepancy between theory and experiment for both gold and aluminum also appears to exist for low photon energies ($k=20$ keV) for the case of both the electron and photon being emitted at 30° .

I. INTRODUCTION

One of the possible modes of interaction of an electron with an atom is the inelastic scattering process known as atomic-field bremsstrahlung production. This fundamental process involves the sudden acceleration of an electron by the electric field of an atom, accompanied by the simultaneous emission of a photon. Since the recoil atom is massive compared to the electron, the amount of energy it receives from the incoming electron may be neglected. Thus, the sum of the energy of the scattered electron and the energy of the photon must equal that of the incident electron. Since the recoil atom does have a non-negligible amount of momentum, however, the photon may be radiated in any direction, regardless of the direction of the scattered electron. For a large number of electrons impinging upon matter, there will be, in effect, a continuous distribution of electromagnetic radiation emitted in all directions, ranging in energy from zero to the energy of the incident electron.

The experiment reported here consisted of a coincidence measurement of the absolute cross section for the fundamental atomic-field bremsstrahlung process, including its dependence upon the electron- and photon-emission angles and the photon energy. This triply differential cross section is denoted by $d^3\sigma/dk d\Omega_k d\Omega_e$, where σ is the cross section, k is the photon energy, and Ω_k and Ω_e are the photon and electron solid angles, respectively. (In this paper this quantity will be called the fully differential cross section, although it might be noted that the formulas and measurements are summed or averaged over the direc-

tions of the electron spins and the photon polarization, and thus that the quantity is not completely differential in a technical sense.) A schematic of the definitions of the angles involved in the bremsstrahlung process is shown in Fig. 1. The results of the experiment are herein compared with the two available fully differential cross-section calculations. Such a comparison is useful in general because it can serve as a test for the applicability of various models and approximations used in nonexact quantum-mechanical calculations. For example, it affords a test of the accuracy of various wave functions commonly used in theoretical work, such as, in the simplest case, the use of a plane wave in the Born approximation. Also, it can provide a test of the validity of the various models used for making electron screening corrections, such as the form-factor approach using the Thomas-Fermi model of the atom. And, in cases where calculations are available, it can serve as a test of the fundamental theory of quantum electrodynamics itself.

A coincidence measurement of the fully differential cross section is preferable to a simple measurement of the doubly or singly differential cross section in which the electron angle or photon energy or both have been integrated over for at least two reasons. First, the coincidence measurement does not suffer from the background subtraction problem which has been a serious difficulty in the measurement of continuous distributions such as bremsstrahlung, since the background spectrum has approximately the same shape as the spectrum being investigated. Second, the fully differential cross section furnishes a sensitive check of the theoretical work in its barest form, with

no spatial or energy integrations to cover-up the fundamental behavior of the process.

The disadvantages of a coincidence measurement are lower counting rate and the general difficulty of making coincidence measurements, especially at low energies. Therefore, although a coincidence measurement of the bremsstrahlung cross section had been suggested as early as 1932,¹ none had been performed at the time the preliminary steps for the present work were undertaken in 1966.

II. BACKGROUND

A. Theoretical

The status of electron-bremsstrahlung cross sections as of 1959, both theoretical and experimental, was summarized in a review paper by Koch and Motz.² From this paper it can be seen that, at that time, there existed several formulas for the doubly differential and singly differential cross sections but, for all practical purposes, only two formulas for the fully differential case. This situation remained unchanged until 1969; however, since that time, at least three more calculations have been published, each at an increased level of sophistication.

The earliest important theoretical bremsstrahlung calculation was a relativistic Born approximation derived in varying form by Bethe and Heitler,³ Sauter,⁴ and Racah.⁵ The result, now known as the Bethe-Heitler formula, is usually considered as being valid only for low atomic number of the scattering atom and for high energies. The region of validity is commonly stated in a rough form as $\alpha Z/\beta_0 \ll 1$ and $\alpha Z/\beta \ll 1$, where α is the fine-structure constant, Z is the atomic number of the scattering atom, and $\beta_0(\beta)$ is the ratio of the velocity of the incident (scattered) electron to that of light. The Bethe-Heitler result usually includes electron screening effects by the use of a correction factor which is applied at the end of the cross-section calculation. This correction is obtained by the well-known method of the form-factor approach based upon a Born approximation. The most common method of

determining this form factor is through the use of the Molière potential function for the Thomas-Fermi-model atom.²

A supposedly more-correct bremsstrahlung cross-section derivation was done by Elwert,⁶ and later modified and numerically evaluated by Haug.^{7,8} The Elwert-Haug procedure used Sommerfeld-Maue⁹ wave functions for the electron continuum. These are relativistic point Coulomb wave functions, valid up to order αZ . Therefore, the region of validity of the Elwert-Haug result is approximately given by $\alpha Z \ll 1$, indicating that the calculation is expected to be valid for all energy ranges, but only for low atomic number.

Deck, Moroi, and Alling¹⁰ have also derived a formula for the fully differential bremsstrahlung cross section using modified Sommerfeld-Maue wave functions. The result is essentially equivalent to a second Born approximation and leads to a correction term of order αZ which is added to the Bethe-Heitler formula. The region of validity is expected to be the same as that of the Bethe-Heitler equation.

Simplified calculations using Sommerfeld-Maue wave functions in the extreme relativistic region (above 50 MeV) have been carried out by Olsen, Maximon, and Wergeland.¹¹ The final form of these calculations is simply that of the Bethe-Heitler formula plus an additive correction.

An exact calculation using the method of partial waves has been done by Tseng and Pratt.¹² Their procedure made use of four different models for the atomic potential (three screened potentials and a point Coulomb potential without screening), which allowed them to investigate the effect of atomic electron screening. Their results have been integrated over the outgoing electron angle, and hence no comparison can be made with other fully differential cross sections. However, their results do indicate that, in general, where screening is significant, the form-factor approach is not adequate. Since the screening is very sensitive to the factor k/T_0 (where T_0 is the incident electron energy), increasing as k/T_0 becomes less, the type of work presented here could be of help in checking the validity of their findings.

As suggested above, at the time the present experiment was initiated in 1966, most of the experimental and theoretical work that had been published was for the cases of singly or doubly differential cross sections. There existed, at that time, severe discrepancies between theory and experiment, particularly in three regions: (1) large atomic number, (2) large values of the ratio k/T_0 , and (3) large photon scattering angle.² Since that time, however, most of the disagree-

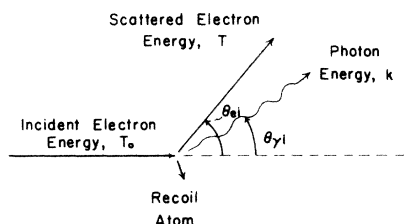


FIG. 1. Definitions of angles involved in the bremsstrahlung process.

ment seems to have been resolved by the more sophisticated calculations, particularly those of Tseng and Pratt.¹² For both $Z = 13$ and $Z = 79$ the modified Hartree-Fock-Slater screened potential results of Tseng and Pratt appear to give good agreement with the experimental data of Aiginger,^{13,14} Rester and Dance,¹⁵ and Rester^{12,16} for the incident energy range 0.050–1 MeV, and with Heroy¹⁷ at 0.050 MeV. The agreement is less good, however, with the older data of Motz¹⁸ and Motz and Placious¹⁹ for the same energy range. The only apparent discrepancies with the above-mentioned data of Aiginger, Rester, and Rester and Dance appear to be in a few cases at small photon angles; hence, it can be concluded that there is generally reasonable agreement between experiment and theory for the doubly differential case.

B. Experimental

In the period since 1966, there have appeared several results of measurements of fully differential bremsstrahlung cross sections, although none have been very extensive. By the end of 1967, two relative photon angular distribution measurements for 300-keV electrons incident on Al and Au with $k = 130$ keV ($k/T_0 = 0.43$) had been reported by Nakel,^{20–22} and an electron relative angular distribution for 300-keV electrons incident on Al with $k = 80$ keV ($k/T_0 = 0.27$) had been reported by Hub and Nakel.²³ For the most part, these measurements agreed qualitatively with the calculations of Elwert and Haug.

In 1969 two high-energy wide-angle absolute cross-section points were reported, one at an incident energy of 900 MeV by Bernardini *et al.*,²⁴ and one at an incident electron energy of 2.5 to 9.5 GeV by Siemann *et al.*²⁵ Both of these experiments were designed to test the theory of quantum electrodynamics in the extreme relativistic region and for low Z , in which instance the Bethe-Heitler formula is expected to be exact. Both experiments gave satisfactory agreement with theory with an experimental uncertainty of

about 10%.

In the period 1970–1971 the first absolute measurements of the fully differential cross section at low energies were reported by Nakel and co-workers.^{26,27} There were two published reports, one²⁶ of a measurement at a single kinematic point for 300-keV electrons incident on Al with $k = 100$ keV ($k/T_0 = 0.33$), and one²⁷ of a measurement repeated at the same kinematic point for Au. The aluminum result was in excellent agreement with the calculation of Elwert-Haug, while the gold result was about 40% higher (with a standard deviation of 25%) than the Elwert-Haug prediction. The gold result, however, gave even worse agreement with the Deck-Moroi-Alling calculation and with what was denoted as the first Born approximation.

In 1972 a more detailed investigation of the absolute cross section was reported by Aehlig and Scheer.²⁸ They measured a photon distribution for 180-keV electrons incident on silver with $k = 80$ keV ($k/T_0 = 0.44$) and a forward electron scattering angle of 30° . Their results, in general, were in agreement with Elwert-Haug within the experimental uncertainties, in slight disagreement with Bethe-Heitler, and in large disagreement with Deck-Moroi-Alling. (A summary of the kinematic values for all the absolute measurements is given in Table I.)

Thus, the results given in this work for gold and aluminum over a wide range of kinematic points represent the most extensive investigation of the fully differential cross section yet presented.²⁹ (See Table I for the exact points investigated.) Furthermore, these results represent the lowest energy range investigated to date, not only with respect to the incident energy T_0 and photon energy k , but also with respect to the important quantity, k/T_0 .

III. EXPERIMENT

The cross section as measured in the present experiment was determined from

TABLE I. Summary of the kinematic points for which absolute measurements of $d^3\sigma/dk d\Omega_k d\Omega_e$ have been made.

| T_0 | Z | θ_{ei} (deg) | θ_{yi} (deg) | k/T_0 | Ref. |
|-------------|--------|------------------------|------------------------|-----------|----------------------------------|
| 2.5–9.5 GeV | 6 | –6.4 | 6.2 | 0.5 | Siemann <i>et al.</i> (1969) |
| 900 MeV | 1 | 25.7, 26.5 | 25.7, 26.5 | 0.5 | Bernardini <i>et al.</i> (1969) |
| 300 keV | 13, 79 | 0 | 13 | 0.33 | Nakel <i>et al.</i> (1969, 1971) |
| 180 keV | 47 | 30 | –75 to 55 | 0.45 | Aehlig and Sheer (1972) |
| 140 keV | 13, 79 | 15 | 270 | 0.21, 0.5 | Present experiment |
| | | 30 | 270 | 0.14, 0.5 | |
| | | 30 | 30 | 0.14, 0.5 | |

$$\frac{d^3\sigma}{dk d\Omega_k d\Omega_e} = \frac{N_c}{N_0 \Delta k \tau \epsilon_e \Delta\Omega_e \epsilon_r \Delta\Omega_r},$$

where N_c is the number of electron-photon coincidences recorded, N_0 is the number of electrons incident upon the target, Δk is the width of the accepted photon energy window, and τ is the effective target thickness. The electron solid angle is $\Delta\Omega_e$ and the combined electron-spectrometer-detector efficiency is ϵ_e ; likewise $\Delta\Omega_r$ is the photon-detector solid angle and ϵ_r is the photon-detector efficiency.

A. General procedure

Electrons with energy of 140 keV from a linear accelerator were directed upon thin targets of aluminum and gold mounted in a 2-in.-diam aluminum scattering chamber. The electron-beam diameter at the target was $\frac{1}{16}$ in. The number of electron-bremsstrahlung events, N_c , was then measured by detecting the scattered electron and bremsstrahlung photon in coincidence. A fast-slow coincidence system was used to provide both timing and energy analysis. All measurements were made in the scattering plane, i.e., $\phi = 0^\circ$, where ϕ is the angle between the plane defined by the incident beam and the outgoing photon, and the plane defined by the incident beam and the outgoing scattered electron. A diagram of the experimental setup is shown in Fig. 2.

B. Electron detector

The scattered electrons were detected by a surface-barrier silicon detector mounted in a mag-

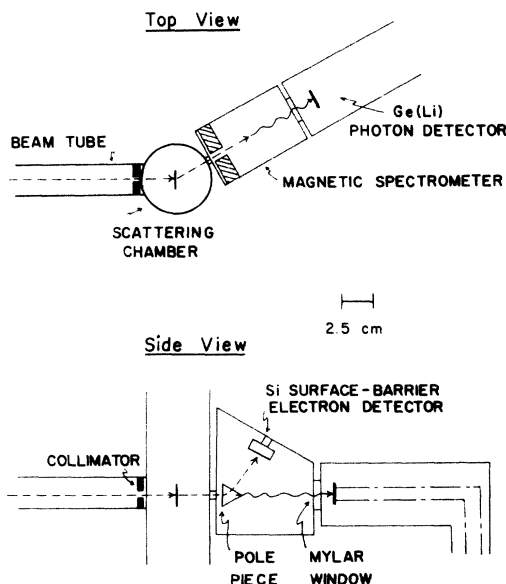


FIG. 2. Schematic view of the experimental layout.

netic electron spectrometer which was positioned at an angle of either 15° or 30° with respect to the incident beam. The purpose of the spectrometer was to separate the inelastically scattered electrons resulting from the bremsstrahlung process from the elastically scattered electrons. This was necessary since the latter outnumbered the former by several orders of magnitude. The electron detector had an energy resolution of 15 keV full width at half-maximum (FWHM) at 70 keV, while the resolution of the electron spectrometer was about 18 keV FWHM at 70 keV. The collimating aperture for the electron spectrometer was circular with a total angular width of about 5° . The spectrometer-detector combination subtended an effective solid angle of about 0.003 sr.

C. Photon detector

The bremsstrahlung photons were detected by a liquid-nitrogen-cooled Ge(Li) detector with an energy resolution of 1.4 keV FWHM at 60 keV. The photon detector was positioned either at the same angle as the electron spectrometer, or at 270° , but was located outside the vacuum system. When both detectors were at the same angle ($\theta_{ei} = \theta_{yi} = 30^\circ$, which is the case shown in Fig. 2) a Mylar window in the rear of the magnetic spectrometer allowed photons to pass through the spectrometer and into the photon detector, with very little attenuation. Otherwise, when the photon detector was at 270° , a Mylar window in the side of the scattering chamber was used. The photon-collimating aperture was circular with an angular acceptance of about 5° or less and a solid angle of approximately 0.0004 sr at the 30° position and about 0.02 sr at the 270° position.

D. Electronics

The pulses from both detector preamps were routed to a fast-slow coincidence system with a timing resolution of 27 nsec FWHM. A block diagram of the system is shown in Fig. 3. The fast coincidence circuit consisted of two timing filter amplifiers, two constant fraction discriminators, a gate and delay generator (which merely served as a variable delay), and time-to-amplitude converter. The pulses from the time-to-amplitude converter were fed to a 1024-channel pulse-height analyzer. The slow coincidence circuit consisted of two linear amplifiers, two timing single-channel analyzers, and a diode slow coincidence unit. The output from the slow coincidence unit was used to gate the pulse-height analyzer, thus providing the energy-analysis part of the experiment.

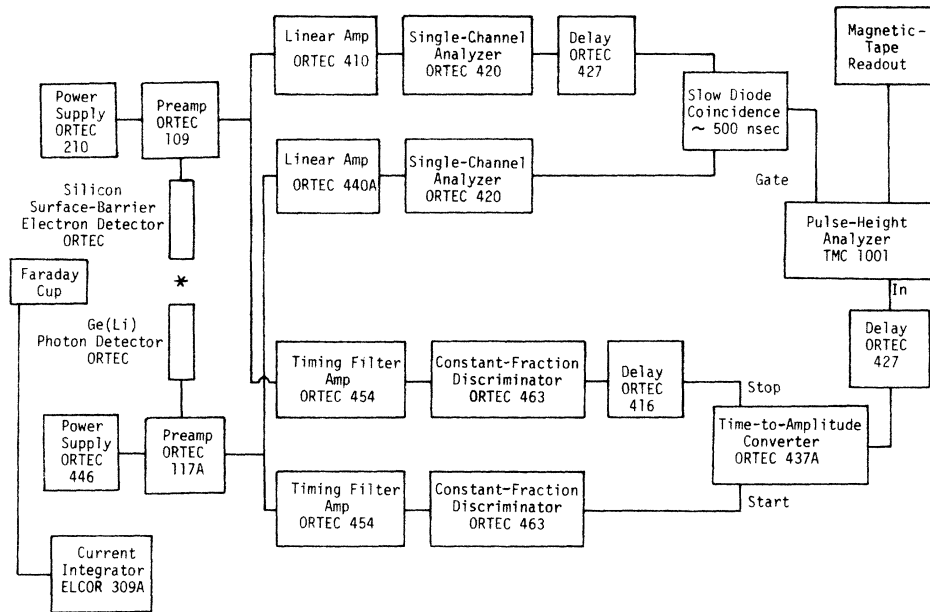


FIG. 3. Block diagram of the electronics.

E. Determination of number of coincidences

The data-accumulation time for a single run ranged from about 5 to 36 h. Each measurement at a particular kinematic point was performed at least twice to check for consistency. To lower the statistical uncertainty, measurements at some points were repeated up to five times. A typical timing peak (partially computer plotted) is shown in Fig. 4 for a 31-h run on a $32.5\text{-}\mu\text{g}/\text{cm}^2$ gold target. The number of actual coincidences, N_c , was determined by using a simple computer program to integrate the timing peak and to subtract the flat background of random coincidences that lie beneath the peak.

F. Determination of energy window

The energy window, Δk , was established by the photon single-channel analyzer. The photon channel was selected for this purpose because of the better energy resolution of the photon detector. Radioactive sources of Co^{57} , Cd^{109} , and Am^{241} were used for the energy calibration, providing calibration points at 14.4, 22.6, 59.5, and 88.0 keV. The window, Δk , was adjusted to have a width of approximately 10 keV and was accurately measured for each run. Depending upon the kinematic point being measured, the center of the window was set for either 20, 30, 50, or 70 keV. The energy window in the electron single-channel analyzer was set much wider than the window in the photon side, thus ensuring that the photon energy window was the determining one for the Δk needed for the calculations.

G. Determination of incident charge

The incident electron intensity was measured by moving a carbon Faraday cup into the path of the beam. The Faraday cup was connected to a current integrator that was capable of accurately measuring currents as low as 10^{-11} A. The total number of electrons incident on the target, N_0 , was measured by integrating throughout the run the charge accumulated on a carbon shield which lined most of the scattering chamber. At the start or end of a data-accumulation run the carbon Faraday cup was moved into the path of the beam and a value found for the ratio of the actual beam

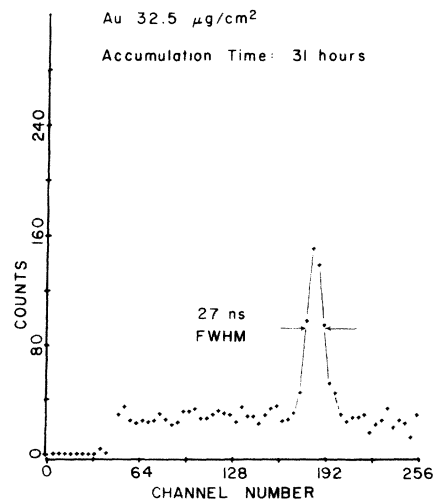


FIG. 4. A typical timing spectrum showing the coincidence peak.

intensity to the beam intensity as measured by the carbon shield. The carbon shield also served a secondary purpose by reducing the production of high-energy bremsstrahlung in the aluminum walls of the scattering chamber.

H. Fabrication of targets

The thin targets were made by vapor deposition of the metal upon glass slides coated with a dilute soap solution. The thin layers were then floated upon water and picked up on aluminum target frames. The gold targets were deposited on thin carbon backings, while the aluminum targets were self-supporting. The thickness of the targets was measured by a weighing technique which gave about 5% accuracy. This target preparation and weighing technique has been described in more detail by Heroy.¹⁷ The targets were mounted in the scattering chamber either perpendicular to the incident beam or at an angle of 30° from the perpendicular position. The target frame holder contained two targets plus the Faraday cup and could be moved vertically while the scattering chamber was evacuated. Thus, the targets could be changed (i.e., a gold target moved out of the beam path and an aluminum target moved in) without bringing the chamber up to atmospheric pressure.

I. Determination of target thickness and electron-detector efficiency—solid angle

To lessen the inaccuracies that would arise in trying to independently determine target thickness, electron-detector solid angle, and electron-detector and magnetic spectrometer efficiency, the product of these quantities was measured. This was accomplished by performing a measurement of the number of electrons elastically scattered at the energy of interest (120, 110, 90, or 70 keV) for a measured incident charge, and then calculating the above-mentioned factor $\tau \Delta \Omega_e \epsilon_e$ through the use of theoretical differential cross sections for the elastic scattering of electrons. Because of the variation of the transmission of the magnetic spectrometer with electron energy, the target-thickness—electron solid-angle factor was evaluated for both the center and for the end points of the effective electron energy region (established by the photon energy window) and the average of the factor over this energy region determined. For example, if the energy region of 25 to 35 keV was established by the photon window, then the average of the target-thickness—electron solid-angle factor was found over the electron energy region of 105 to 115 keV.

The electron elastic scattering calculations of Moore and Fink^{30,31} were used for gold, and those of Doggett and Spencer³² were used for aluminum. Therefore, all the results presented in this paper have, in effect, been normalized to the results of Moore and Fink or Doggett and Spencer. The calculations for gold of Moore and Fink were chosen because they agree with the accurate experimental results of Kessler and Weichert³³ to within 2%. The calculations for aluminum are also expected to be accurate since, because of the low atomic number, the results are only slightly different from those predicted by Rutherford scattering and screening may be neglected.

J. Determination of photon-detector efficiency and solid angle

The photon-detector solid angle and efficiency were measured as a single factor by placing accurately calibrated radioactive sources at the position in the scattering chamber where the electron beam normally struck the target. This procedure eliminated the necessity for accurately determining the photon-detector solid angle, and in addition, bypassed any geometric effects that might alter the effective photon-detector efficiency. These geometric effects are caused by non-uniformity of the semiconductor wafer with respect to photon detection efficiency; i.e., the detection efficiency varies according to the particular area of the wafer exposed to the photon source. These variations were eliminated by measuring the efficiency in the exact experimental setup. The radionuclides used in the measurement were Cd¹⁰⁹, which provided *K* x-rays at 22.6 keV and γ rays at 88.0 keV, and Am²⁴¹, which emitted γ rays at 59.5 keV. The Cd¹⁰⁹ source was supplied with its activity measured in terms of emission of the 88.0-keV γ ray. A *K* x-ray-to- γ -ray intensity ratio of 25.9 (Refs. 34 and 35) was used to obtain the intensity of the *K* x-ray emission. The Am²⁴¹ radioactive source was calibrated in disintegrations per second and an intensity value of 0.353 (Ref. 36) was used for the 59.5-keV γ ray. Photon efficiencies for the energies of interest in the experiment were then obtained by interpolation. This process was aided by knowledge of the approximate general shape of the efficiency curve for the Ge(Li) detector. This had previously been determined by the use of a wide assortment of accurately calibrated radioactive sources with photon emission in the 6–166-keV range. The details of this efficiency curve determination have been discussed by Davis³⁷ and by Faulk and Quarles.³⁸

K. Experimental checks

1. Correlated noise pulses

As a check for coincidences due to correlated noise pulses, measurements were also made with the photon window detuned, i.e., set for an energy region that was kinematically incorrect with respect to the electron energy region established by the electron spectrometer. No real coincidences were observed.

2. Magnetic field effects

To prevent the magnetic field of the spectrometer from distorting the paths of the electrons, several layers of magnetic shielding were placed around the scattering chamber. To check for magnetic field effects, cross-section measurements were made with the spectrometer rotated 30° about the axis defined by the incoming electrons. The measurement was then repeated with the spectrometer rotated 30° to the other side. In both cases no large effects outside the statistical uncertainty were noticed. The magnetic field inside the scattering chamber was also measured directly using a gaussmeter and the paths of the electrons determined by ray tracing. This procedure suggested that the residual magnetic field had negligible effect on the electron paths and, thus, on the cross-section measurements.

3. Multiple scattering effects

To investigate the effect of target thickness upon the cross section measurements (as a check for

possible multiple scattering), cross-section measurements were made for gold targets of approximate thicknesses of 32.5, 60, and 84 $\mu\text{g}/\text{cm}^2$. No difference outside the statistical uncertainty was noted between the 32.5- and 60- $\mu\text{g}/\text{cm}^2$ targets; however, the 84- $\mu\text{g}/\text{cm}^2$ measurement seemed to be slightly disturbed by multiple scattering. These results are in rough agreement with those of Kreuzer and Nakel.²⁷ Measurements were also made using 60- and 84- $\mu\text{g}/\text{cm}^2$ targets of aluminum. No noticeable difference was observed in this case.

IV. RESULTS

The results of the present investigation are shown in Figs. 5 through 10. The experimental cross-section measurements are plotted as a function of photon energy, with the photon emission angle, the electron scattering angle, and the atomic number of the scattering material used as parameters. Also shown are the theoretical predictions of the Bethe-Heitler² and Elwert-Haug⁸ formulas. The Bethe-Heitler cross-section formula was computed on a programable desk calculator, while the Elwert-Haug formula was evaluated on an IBM 1800 computer. The screening form-factor correction applied to the Bethe-Heitler and Elwert-Haug calculations was computed using the Molière potential function for the Thomas-Fermi-model atom. The potential function and the values for the constants contained

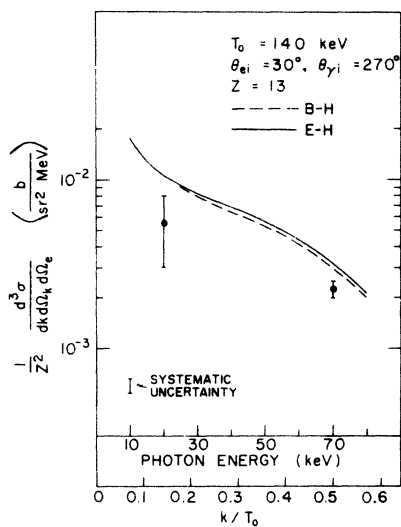


FIG. 5. The differential cross section for aluminum for $\theta_{ei} = 30^\circ$ and $\theta_{\gamma i} = 270^\circ$ vs photon energy and k/T_0 . The curves are the evaluations of the Bethe-Heitler and the Elwert-Haug formulas.

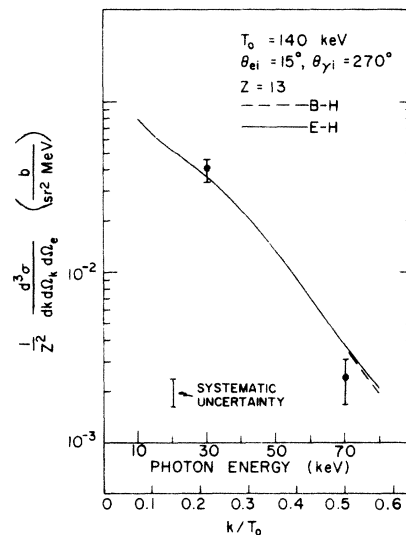


FIG. 6. The differential cross section for aluminum for $\theta_{ei} = 15^\circ$ and $\theta_{\gamma i} = 270^\circ$ vs photon energy and k/T_0 . The curves are the evaluation of the Bethe-Heitler and the Elwert-Haug formulas.

therein were taken from the review paper of Koch and Motz.²

A. Uncertainties

The error bars on the experimental data points represent the random uncertainties associated with the individual points. At an estimated level of one standard deviation, they were typically as follows: coincidence counts, 11%; current integration, 1%; photon window, 2%; electron solid-angle-target-thickness factor, 5%; and relative photon efficiency, 2%. The resultant total random uncertainty was obtained by combining the above quantities in quadrature.

The error bars shown at the bottom of the figures represent the estimated total systematic uncertainty at about the one standard-deviation level. "Systematic" in this case implies that the uncertainty does not vary either from run to run or with photon energy. In other words, for any one particular graph this uncertainty remains constant for all the data points contained thereon. The total systematic uncertainty was observed by combining in quadrature the individual systematic uncertainties, which were typically as follows: current integration, 1%; electron solid-angle-target-thickness factor, 4 to 16%; and photon efficiency-solid angle, 8%.

The large systematic uncertainty for the electron solid-angle-target-thickness factor derives from an absolute uncertainty of $\pm 1^\circ$ in the angular position of the electron spectrometer. For ex-

ample, at $\theta_{ei} = 15^\circ$ this uncertainty in the angle leads to a large possible error in the value of the elastic scattering cross section [due to the approximately $\sin^4(\theta/2)$ dependence of the cross section] used in calculation of the electron solid-angle-target thickness factor, which, in turn, leads to a large possible error in the factor itself. At $\theta_{ei} = 30^\circ$ the effect was much less.

No corrections were made to the theoretical bremsstrahlung cross sections for the finite solid angles and energy windows used in the experiment. The average value of the Bethe-Heitler cross section over these finite angular and energy widths was checked for different kinematic points and the resultant found to be within 1% of the theoretical value at the central point. Some correction in the experimental data had to be made, however, for $\theta_{ei} = 15^\circ$ because of the finite width of the electron-spectrometer aperture. This correction was again due to the strong angular dependence of the elastic scattering cross section which affected the resultant value determined for the electron solid-angle-target-thickness factor. No correction due to finite widths was needed for $\theta_{ei} = 30^\circ$.

B. Discussion of results for $Z=13$

The results of the experimental measurements for aluminum are shown in Figs. 5-7. For the backward-photon-angle case of $\theta_{ei} = 30^\circ$ and $\theta_{\gamma i} = 270^\circ$, as shown in Fig. 5, the theoretical calculations are too close in agreement for any type of distinction to be made. Taking the total uncertainty into account, the experimental points lie

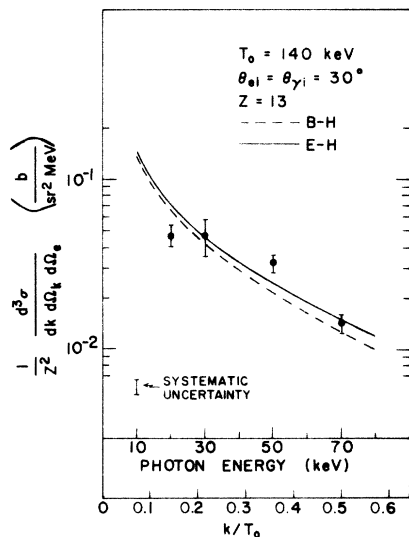


FIG. 7. The differential cross section for aluminum for $\theta_{ei} = \theta_{\gamma i} = 30^\circ$ vs photon energy and k/T_0 . The curves are the evaluation of the Bethe-Heitler and the Elwert-Haug formulas.

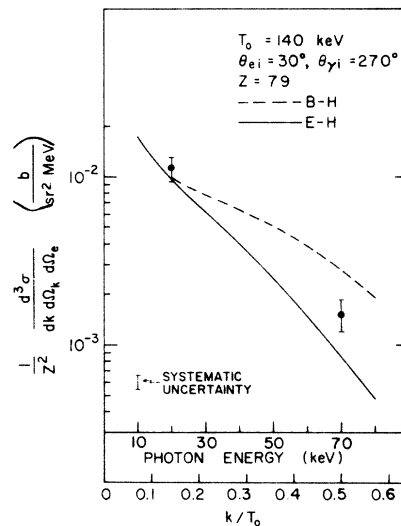


FIG. 8. The differential cross section for gold for $\theta_{ei} = 30^\circ$ and $\theta_{\gamma i} = 270^\circ$ vs photon energy and k/T_0 . The curves are the evaluation of the Bethe-Heitler and Elwert-Haug formulas.

barely below one standard deviation from both calculations. The results for $\theta_{ei} = 15^\circ$ and $\theta_{\gamma i} = 270^\circ$ are shown in Fig. 6. As can be seen, there is relatively good agreement with both theories. Again the theoretical values are too close to really distinguish between the two. The results for the forward-photon-angle case of $\theta_{ei} = \theta_{\gamma i} = 30^\circ$ are shown in Fig. 8. Here, there appears to be some disagreement with the theoretical curves. The data at 50-keV photon energy appear high and the data at 20 keV appear low. While this could indicate a disagreement with the shape of the theoretical curve over the entire energy range, the more likely explanation, considering the systematic error, seems to be that the datum point at low photon energy is unusually low. This discrepancy at low photon energy is also observed for gold and will be discussed further.

C. Discussion of results for $Z=79$

The results for gold are shown in Figs. 8–10. For the backward-angle case of $\theta_{ei} = 30^\circ$ and $\theta_{\gamma i} = 270^\circ$ the results are mixed. The 20-keV point agrees with both theories (there again being very little difference between the numerical values of the two calculations at this point) and the 70-keV point lies about midway between the two theories, in disagreement with both. Clearly, this would be a good point for which to evaluate the exact calculation of Tseng and Pratt for comparison; and it is hoped that such an evaluation will be available at some future date. For the other backward-

angle case of $\theta_{ei} = 15^\circ$ and $\theta_{\gamma i} = 270^\circ$, as shown in Fig. 9, the results favor the Elwert-Haug theory, particularly at 30 keV.

The gold results for the forward-photon-angle case of $\theta_{ei} = \theta_{\gamma i} = 30^\circ$ are shown in Fig. 10. Over all, it can be said that the experimental data generally agree with both calculations. However, there does appear to be a disagreement with both theories at the lowest photon energy of 20 keV ($k/T_0 = 0.14$). This is similar to the situation observed for aluminum at this angular position. As a check on this rather surprising result, this point was remeasured for gold using a liquid-nitrogen-cooled Si(Li) photon detector in place of the Ge(Li) detector. The two results agree with each other when the systematic uncertainty is included, but both disagree (as measured by arithmetical addition of the systematic and random uncertainties) with the theoretical calculations. This disagreement might be taken to be due to inadequate theoretical treatment of screening effects, except that the same result occurs for aluminum, for which screening should be relatively unimportant. The deviation might be due to some overlooked photon-energy-dependent error in the experiment; however, after much checking none was found. Further, there was good agreement for gold at the backward photon angle of 270° for the 20-keV point. Perhaps the random uncertainties have been underestimated, but we do not believe this to be the case. Certainly it would also be interesting to have an evaluation of the exact cal-

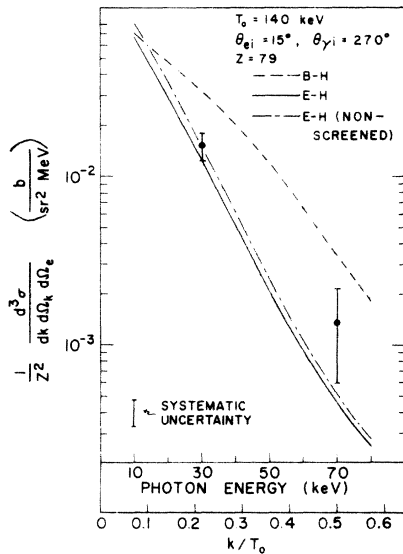


FIG. 9. The differential cross section for gold for $\theta_{ei} = 15^\circ$ and $\theta_{\gamma i} = 270^\circ$ vs photon energy and k/T_0 . The curves are evaluations of the Bethe-Heitler and the screened and unscreened Elwert-Haug formulas.

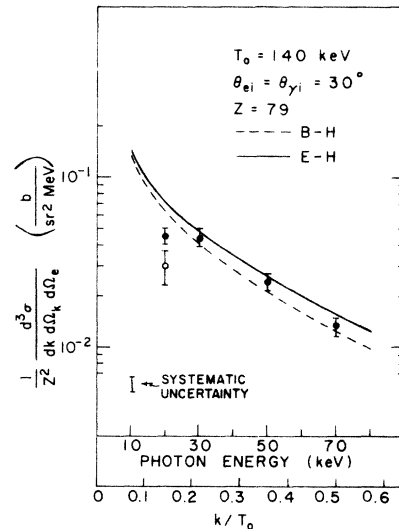


FIG. 10. The differential cross section for gold for $\theta_{ei} = \theta_{\gamma i} = 30^\circ$ vs photon energy and k/T_0 . The datum point at $k = 70$ keV, shown by the open circle, was taken with a Si(Li) detector. The curves are the evaluation of the Bethe-Heitler and the Elwert-Haug formulas.

calculation of Tseng and Pratt for this low-photon-energy point. However, due to the excessive number of partial waves which would have to be included and the consequent computer time, such an evaluation does not appear feasible.

V. CONCLUSIONS

In conclusion, for low atomic number ($Z=13$) both the Bethe-Heitler and the Elwert-Haug calculations agree reasonably well with the experimental results over the photon energy range except for the forward-angle low-photon-energy case discussed above. This agreement is not surprising for the Elwert-Haug formula, since its region of validity is for low Z and is not dependent upon the energy. However, the agreement may be somewhat unexpected for the Bethe-Heitler formula whose accuracy does depend upon the energy. Of course, in this case both formulas agree well with each other, so we can conclude that the Bethe-Heitler formula is still accurate at low Z for an incident energy of 140 keV and for scattered electron energy as low as 70 keV.

For high atomic number ($Z=79$), where neither cross-section calculation is really expected to be valid, both calculations seem to agree with experiment at the forward photon angle (except for the 20-keV point, as already discussed), while the Elwert-Haug calculation seems to be favored at the backward photon angle, particularly for $\theta_{ei}=15^\circ$. However, even this calculation fails noticeably at the high-photon-energy backward-angle point, especially for $\theta_{ei}=30^\circ$. Also, it might be pointed out that the two theoretical cal-

culations differ only slightly at high electron (i.e., low photon) energies and agree reasonably well with experiment at these points (again, except for the 20-keV forward-angle point). This indicates that the Bethe-Heitler and the Elwert-Haug calculations are accurate to a significant degree, even for high Z , when the incident and scattered electrons have energies of about 100 keV.

With respect to screening, it should be noted that the experiment will have to be improved before any definite results can be obtained in this area. To illustrate this point, the unscreened Elwert-Haug result has been shown in Fig. 9. According to the Thomas-Fermi-Molière screening calculation, it is in this kinematic region (out of those investigated in the present experiment) that atomic electron screening has its largest effect. The small relative difference between the screened and unscreened cases illustrates the difficulty in making a significant test of how well screening is really accounted for by current theoretical methods.

ACKNOWLEDGMENTS

The authors wish to acknowledge Dr. Leo Baggerly for suggesting this area of research, Dr. Nat Edmonson for his interest and support during the early phase of the work, and Jim Williams and Steve Murdock for assistance with construction of much of the apparatus. We wish to thank Dr. Tseng for helpful comments and for providing us with some evaluations of the Elwert-Haug formula before our own program was completed.

*Work supported in part by NASA under Contract Nos. NAS 8-21421 and NAS 8-24658 and by the TCU Research Foundation.

¹O. Scherzer, *Ann. Phys. (Leipz.)* **13**, 137 (1932).

²H. W. Koch and J. W. Motz, *Rev. Mod. Phys.* **31**, 920 (1959).

³H. Bethe and W. Heitler, *Proc. Roy. Soc. Lond. A* **146**, 83 (1934).

⁴F. Sauter, *Ann. Phys. (Leipz.)* **20**, 404 (1934).

⁵G. Racah, *Nuovo Cimento* **11**, 469 (1934).

⁶G. Elwert, dissertation (University of Munich, W. Germany, 1939); published in part in *Ann. Phys. (Leipz.)* **34**, 178 (1939).

⁷E. Haug, dissertation (University of Tubingen, W. Germany, 1966) (unpublished).

⁸G. Elwert and E. Haug, *Phys. Rev.* **183**, 90 (1969).

⁹A. Sommerfeld and A. W. Maue, *Ann. Phys. (Leipz.)* **22**, 629 (1935).

¹⁰R. T. Deck, D. S. Moroi, and W. R. Alling, *Nucl. Phys. A* **133**, 321 (1969).

¹¹H. Olsen, L. C. Maximon, and H. Wergeland, *Phys.*

Rev. **106**, 27 (1957).

¹²H. K. Tseng and R. H. Pratt, *Phys. Rev. A* **3**, 100 (1971).

¹³H. Aiginger and H. Zinke, *Acta Phys. Austriaca* **23**, 76 (1966).

¹⁴H. Aiginger, *Z. Phys.* **197**, 8 (1966).

¹⁵D. H. Rester and W. E. Dance, *Phys. Rev.* **161**, 85 (1967).

¹⁶D. H. Rester, *Nucl. Phys.* **118**, A129 (1968).

¹⁷D. B. Heroy, dissertation (Texas Christian University, Fort Worth, Tex., 1972) (unpublished).

¹⁸J. W. Motz, *Phys. Rev.* **100**, 1560 (1955).

¹⁹J. W. Motz and R. C. Placious, *Phys. Rev.* **109**, 235 (1958).

²⁰W. Nakel, *Phys. Lett.* **22**, 614 (1966).

²¹W. Nakel, *Phys. Lett.* **25A**, 569 (1967).

²²W. Nakel, *Z. Phys.* **214**, 168 (1968).

²³R. Hub and W. Nakel, *Phys. Lett.* **24A**, 601 (1967).

²⁴C. Bernardini, F. Felicetti, R. Querzoli, V. Silverstrini, and G. Vignola, *Nuovo Cimento Lett.* **1**, 15 (1969).

- ²⁵R. H. Siemann, W. W. Ash, K. Berkelman, D. L. Hartill, C. A. Lichtenstein, and R. M. Littauer, *Phys. Rev. Lett.* 22, 421 (1969).
- ²⁶W. Nakel and U. Sailer, *Phys. Lett.* 31A, 181 (1970).
- ²⁷K. Kreuzer and W. Nakel, *Phys. Lett.* 34A, 407 (1971).
- ²⁸A. Aehlig and S. Scheer, *Z. Phys.* 250, 235 (1972).
- ²⁹Preliminary results have been reported: J. D. Faulk and C. A. Quarles, *Bull. Am. Phys. Soc.* 17, 1200 (1972); J. D. Faulk and C. A. Quarles, *Phys. Lett.* 44A, 317 (1973).
- ³⁰P. Moore and M. Fink, *Phys. Rev. A* 5, 1747 (1972).
- ³¹M. Fink (private communication, 1972).
- ³²J. A. Doggett and L. V. Spencer, *Phys. Rev.* 103, 1597 (1956).
- ³³J. Kessler and N. Weichert, *Z. Phys.* 212, 48 (1968).
- ³⁴H. Leutz, K. Schneckenberger, and H. Wenninger, *Nucl. Phys.* 63, 263 (1965).
- ³⁵J. L. Campbell and L. A. McNelles, *Nucl. Inst. Meth.* 98, 433 (1972).
- ³⁶M. J. Martin and P. H. Blichert-Toft, *Nucl. Data A* 8, 1 (1970).
- ³⁷D. V. Davis, dissertation (Texas Christian University, Fort Worth, Tex., 1971) (unpublished).
- ³⁸J. D. Faulk and C. A. Quarles, *Texas J. Sci.* 24, 372 (1972).